Article:
Matin, T.N., Rahman, N., Nickol, A.H. et al. (2017) Chronic Obstructive Pulmonary Disease: Lobar Analysis with Hyperpolarized 129Xe MR Imaging. Radiology, 282 (3). p. 152299. ISSN: 0033-8419

https://doi.org/10.1148/radiol.2016152299

Radiology

Chronic Obstructive Pulmonary Disease: Lobar Analysis with Hyperpolarized ^{129}Xe MR Imaging[1]

Tahreema N. Matin, MBBS, BSc, FRCR
Najib Rahman, DPhil, MSc, FRCP
Annabel H. Nickol, DPhil, FRCP
Mitchell Chen, DPhil, MBBS
Xiaojun Xu, PhD
Neil J. Stewart, PhD
Tom Doel, DPhil
Vicente Grau, DPhil
James M. Wild, PhD
Fergus V. Gleeson, FRCP, FRCR, FCCP

Purpose: To compare lobar ventilation and apparent diffusion coefficient (ADC) values obtained with hyperpolarized xenon 129 (^{129}Xe) magnetic resonance (MR) imaging to quantitative computed tomography (CT) metrics on a lobar basis and pulmonary function test (PFT) results on a whole-lung basis in patients with chronic obstructive pulmonary disease (COPD).

Materials and Methods: The study was approved by the National Research Ethics Service Committee; written informed consent was obtained from all patients. Twenty-two patients with COPD (Global Initiative for Chronic Obstructive Lung Disease stage II–IV) underwent hyperpolarized ^{129}Xe MR imaging at 1.5 T, quantitative CT, and PFTs. Whole-lung and lobar ^{129}Xe MR imaging parameters were obtained by using automated segmentation of multisection hyperpolarized ^{129}Xe MR ventilation images and hyperpolarized ^{129}Xe MR diffusion-weighted images after coregistration to CT scans. Whole-lung and lobar quantitative CT–derived metrics for emphysema and bronchial wall thickness were calculated. Pearson correlation coefficients were used to evaluate the relationship between imaging measures and PFT results.

Results: Percentage ventilated volume and average ADC at lobar ^{129}Xe MR imaging showed correlation with percentage emphysema at lobar quantitative CT ($r = -0.32$, $P < .001$ and $r = 0.75$, $P < .0001$, respectively). The average ADC at whole-lung ^{129}Xe MR imaging showed moderate correlation with PFT results (percentage predicted transfer factor of the lung for carbon monoxide [T_{LCO}]: $r = -0.61$, $P < .005$) and percentage predicted functional residual capacity ($r = 0.47$, $P < .05$). Whole-lung quantitative CT percentage emphysema also showed statistically significant correlation with percentage predicted T_{LCO} ($r = -0.65$, $P < .005$).

Conclusion: Lobar ventilation and ADC values obtained from hyperpolarized ^{129}Xe MR imaging demonstrated correlation with quantitative CT percentage emphysema on a lobar basis and with PFT results on a whole-lung basis.

[1] From the Department of Radiology (T.N.M., M.C., X.X., F.V.G.) and Oxford Centre for Respiratory Medicine (N.R., A.H.N.), The Churchill Hospital, Oxford University Hospitals NHS Trust, Old Rd, Headington, OX3 7LE, England; Unit of Academic Radiology, Royal Hallamshire Hospital, University of Sheffield, Sheffield, England (N.J.S., J.M.W.); and Institute of Biomedical Engineering, Department of Engineering Science, University of Oxford, Headington, England (T.D., V.G.). Received October 19, 2015; revision requested December 7; revision received April 10, 2016; accepted May 26; final version accepted July 28. **Address correspondence to** T.N.M. (e-mail: *tahreema.matin2@ouh.nhs.uk*).

Supported by the National Institute for Health Research (NIHR) Oxford Biomedical Research Centre Programme and sponsored by the Oxford University Hospitals NHS Trust.

The views expressed are those of the authors and not necessarily those of the NHS, the National Institute for Health Research, or the Department of Health.

Chronic obstructive pulmonary disease (COPD) is a leading cause of morbidity and mortality (1), accounting for a significant economic and social burden worldwide (2). COPD is characterized by progressive airflow limitation caused by a combination of small airways disease (obstructive bronchiolitis) and parenchymal destruction (emphysema) (1).

The standard method for assessing lung function in COPD is spirometry, which, combined with anatomic imaging (computed tomography [CT]), can provide structural information. Spirometry alone provides information on global lung function, and findings do not correlate with patient symptoms or survival (3). The provision of an accurate, robust regional imaging technique that can help quantify heterogeneous disease and treatment responses within different lobes of the lung is needed.

Emerging state-of-the-art functional magnetic resonance (MR) imaging techniques that use gas contrast agents include hyperpolarized gas MR imaging, oxygen-enhanced MR imaging, and fluorinated gas MR imaging. Unfortunately, despite recent advances in gradient performance and sequence acquisition strategy, none of these functional pulmonary MR imaging techniques have been adopted into clinical practice.

MR imaging with hyperpolarized xenon 129 (^{129}Xe) provides a unique strategy for evaluating regional lung function by permitting direct visualization of the lung airspaces. The inherent properties of ^{129}Xe may be exploited to regionally quantify ventilation and diffusion within the lung and enable comprehensive in vivo assessment of lung function. Hyperpolarized ^{129}Xe MR imaging is safe, free from ionizing radiation, and well tolerated in small cohorts of healthy volunteers and patients with COPD who have been imaged to date (4,5).

The pioneering techniques developed to characterize global lung function with use of hyperpolarized helium 3 (^{3}He) MR imaging (6) have been translated to hyperpolarized ^{129}Xe MR imaging (7). Ventilation assessment with hyperpolarized ^{3}He MR imaging has shown utility in the detection of functional abnormalities in a range of obstructive lung abnormalities (eg, COPD, cystic fibrosis, asthma, and bronchiolitis obliterans) (8). High-spatial-resolution imaging of pulmonary ventilation is also possible with hyperpolarized ^{129}Xe MR imaging (4,5,7). With wider availability and lower cost than ^{3}He, ^{129}Xe MR imaging is a more clinically viable alternative and studies have compared ventilation image quality for the two gases (9). Hyperpolarized ^{129}Xe diffusion-weighted MR imaging has also shown utility in the assessment of lung microstructure (7,10), with elevated whole-lung mean apparent diffusion coefficient (ADC) values present in patients with COPD corresponding to emphysematous tissue destruction.

A variety of ventilation scoring metrics have been developed for analysis of ventilation at whole-lung hyperpolarized gas MR imaging, ranging from reader-based scoring (11), manual segmentation (12), and semiautomated segmentation (13) to fully automated segmentation (14). The feasibility of lobar and bronchopulmonary segmental ventilation assessment with hyperpolarized ^{3}He MR imaging has been reported in healthy volunteers and subjects with asthma (15,16). However, methods specifically for lobar quantification of hyperpolarized ^{129}Xe MR imaging ventilation and ADC values in subjects with COPD have not been reported, and it is in these patients that regional analysis may be of benefit when considering their suitability for treatments such as lung volume reduction surgery and endobronchial valve placement. The motivation for this study was to generate lobar measurements of hyperpolarized ^{129}Xe MR imaging–derived ventilation and ADC values by using an automated analysis tool, which could then potentially be incorporated into the clinical workflow for treatment evaluation in patients with obstructive pulmonary disease. The purpose of this study was

Advances in Knowledge

- Lobar ventilation and apparent diffusion coefficient (ADC) values obtained with hyperpolarized xenon 129 (^{129}Xe) MR imaging showed correlation with lobar quantitative CT–derived emphysema ($r = -0.32$, $P < .001$ and $r = 0.75$, $P < .0001$, respectively).
- Whole-lung hyperpolarized ^{129}Xe MR imaging ADC showed correlation with percentage predicted transfer factor of the lung for carbon monoxide ($r = -0.61$, $P < .005$) and percentage predicted functional residual capacity ($r = 0.47$, $P < .05$).

Implication for Patient Care

- In subjects with chronic obstructive pulmonary disease, it is possible to assess lobar contributions to lung function by using hyperpolarized ^{129}Xe MR imaging–derived ventilation and ADC values, and this may be useful in patient selection for pulmonary intervention and treatment monitoring.

Published online before print
10.1148/radiol.2016152299 **Content codes:** CH MR

Radiology 2017; 282:857–868

Abbreviations:
ADC = apparent diffusion coefficient
COPD = chronic obstructive pulmonary disease
FEV_1 = forced expiratory volume in 1 second
FRC = functional residual capacity
%LAA = percentage area with attenuation values less than −950 HU
PFT = pulmonary function test
Pi10 = square root of bronchial wall area for a theoretical airway with an internal perimeter of 10 mm
PTK = Pulmonary Toolkit
T_{LCO} = transfer factor of the lung for carbon monoxide

Author contributions:
Guarantors of integrity of entire study, T.N.M., F.V.G.; study concepts/study design or data acquisition or data analysis/interpretation, all authors; manuscript drafting or manuscript revision for important intellectual content, all authors; manuscript final version approval, all authors; agrees to ensure any questions related to the work are appropriately resolved, all authors; literature research, T.N.M., A.H.N., X.X., J.M.W.; clinical studies, T.N.M., N.R., A.H.N., X.X., J.M.W., F.V.G.; statistical analysis, T.N.M., M.C., X.X.; and manuscript editing, T.N.M., N.R., M.C., V.G., J.M.W., F.V.G.

Conflicts of interest are listed at the end of this article.

to compare hyperpolarized ^{129}Xe MR imaging–derived lobar ventilation and ADC values to quantitative CT metrics on a lobar basis and pulmonary function test (PFT) results on a whole-lung basis in patients with COPD.

Materials and Methods

Subjects

The study was approved by the National Research Ethics Service Committee, and written informed consent was obtained from all patients.

Between July 2013 and January 2015, 22 patients with COPD were prospectively enrolled from a tertiary referral center with the following inclusion criteria: stage II–IV COPD on the basis of Global Initiative for Chronic Obstructive Lung Disease criteria (forced expiratory volume in 1 second [FEV_1] <80% predicted and FEV_1/forced vital capacity <70%), substantial smoking history (>15 pack-years), and age older than 18 years and ability to provide informed consent.

Study exclusion criteria included the presence of coexistent cardiopulmonary disease that predominated over COPD and might confound result interpretation (eg, asthma, bronchiectasis, cystic fibrosis, lung cancer, uncontrolled heart failure, frequent unstable angina, respiratory muscle weakness). During the study period, 15 patients did not fulfill the inclusion criteria: Six patients were classified as having stage I COPD, three patients had a smoking history of less than 15 pack-years, five patients had predominant asthma, and one patient had uncontrolled heart failure.

The final study population included 15 men and seven women (Table 1). The mean patient age (± standard deviation) was 66.6 years ± 7.3 (range, 52–78 years). The mean age of men was 66.7 years ± 7.7 (range, 52–78 years), and the mean age of women was 68.4 years ± 5.2 (range, 57–74 years). There was no significant difference in age between men and women (P = .62, Student t test).

Participants underwent baseline multimodality imaging at a single time point, including hyperpolarized ^{129}Xe MR imaging and quantitative CT. Study measures were obtained during disease stability, which was defined as participants remaining exacerbation free for at least 4 weeks with no change to their regular medications before completion of imaging and PFTs. PFTs and imaging were both completed before bronchodilator treatment to allow for direct comparison. Image analysis was performed by three authors (T.N.M., X.X., and M.C., with 6 years of clinical radiology experience, a PhD in hyperpolarized ^{129}Xe MR imaging, and a PhD in respiratory imaging, respectively) who were blinded to clinical data and PFT results.

^{129}Xe Polarization and Delivery

Isotopically enriched ^{129}Xe gas (80% ^{129}Xe [Spectra Gases, Alpha, NJ, supplied by Littleport, Cambridgeshire, England]) was polarized to 4%–12% by means of rubidium vapor spin-exchange optical pumping and cryogenically accumulated in 1.0-L doses by using a commercial polarizer (Xenospin; Polarean, Durham, NC). Hyperpolarized ^{129}Xe was then thawed into a Tedlar bag (Jensen Inert Products, Coral Springs, Fla) and the polarization was determined by using a polarization measurement station (model 1651; GE Healthcare, Milwaukee, Wis). Hyperpolarized ^{129}Xe was administered by first instructing the subjects, who were lying supine in the MR imaging unit, to exhale to FRC and then inhale the 1.0-L contents of the Tedlar bag through 0.95-cm–inner diameter Tygon tubing (Cole-Palmer Instrument; Hanwell, London, England). Subjects were then instructed to hold their breath for up to 25 seconds for image acquisition. In our experience, patients with COPD are capable of tolerating 25-second breath holds without causing image motion artifacts. Study participants were provided training and instruction for breath-hold imaging, performing practice breath holds beforehand, to ensure that lung volumes were as reproducible as possible for all imaging examinations.

Table 1

Characteristics of Study Population

Parameter	Value
Sex*	
M	15 (68)
F	7 (32)
Mean age (y)	66.6 ± 7.3
Mean pack-years	66.3 ± 47.3
Smoking status*	
Current smoker	8 (36)
Ex-smoker	14 (64)
FEV_1 (L)†	54 ± 17.3
FEV_1/FVC (%)	43.0 ± 11.0
RV/TLC (%)	52.7 ± 9.4
FRC (L)†	149.5 ± 26.9
T_{LCO} (mmol/min/kPa)†	56.7 ± 16.9
GOLD stage*	
II	13 (59.1)
III	8 (36.4)
IV	1 (4.5)
Median %LAA‡	6.4 (1.6, 15.5)
Pi10 (mm)	6.2 ± 0.8
^{129}Xe MR imaging–derived ventilated volume (%)	72.5 ± 14.5
^{129}Xe MR imaging–derived average ADC ($\times 10^{-6}$ m^2/sec)	5.2 ± 1.4§

Note.—Except where indicated, data are means ± standard deviations. FEV_1 is the prebronchodilator value, FRC = functional residual capacity, FVC = forced expiratory vital capacity, GOLD = Global Initiative for Chronic Obstructive Lung Disease, %LAA = percentage area with attenuation values less than −950 HU, given as median (and 25th and/75th percentiles), Pi10 = square root of bronchial wall area for a theoretical airway with an internal perimeter of 10 mm, RV/TLC = residual volume expressed as percentage of total lung capacity, T_{LCO} = transfer factor of the lung for carbon monoxide.

* Data are numbers of patients, with percentages in parentheses.

† Percentage predicted.

‡ Numbers in parentheses are the 25th and 75th percentiles.

§ Data are available for only 21 patients.

MR Imaging

All MR images were obtained with a 1.5-T whole-body system (Signa HDx; GE Healthcare). Subjects were fitted with a flexible twin Helmholtz quadrature transmit-receive coil (Clinical MR Solutions, Brookfield, Wis) resonating at the ^{129}Xe Larmour frequency (17.7 MHz). Images were acquired with patients in the supine position. After initial hydrogen 1 (^{1}H) MR localizer images

were obtained, hyperpolarized ^{129}Xe MR ventilation images were acquired during a breath hold of approximately 25 seconds in the anteroposterior direction by using a broadbanded two-dimensional spoiled gradient-echo sequence. Imaging parameters were as follows: 15-mm coronal sections covering the whole lung in the anteroposterior direction, 40 × 40-cm field of view, 96 × 96 matrix resolution, 4-kHz bandwidth, 20/4.2 (repetition time msec/echo time msec), and 9° flip angle. Hyperpolarized ^{129}Xe MR diffusion-weighted images were obtained by using an interleaved two-dimensional gradient-echo sequence with two b values (b = 0, 20.855 sec/cm^2). Imaging parameters were as follows: 30-mm coronal sections covering the whole lung in the anteroposterior direction, 40 × 40-cm field of view, 96 × 96 matrix resolution, 4-kHz bandwidth, 20/13.2, and 7° flip angle.

Anatomic proton (conventional ^{1}H) MR images were obtained during a separate 15-second breath hold after both hyperpolarized ^{129}Xe MR ventilation and diffusion-weighted imaging. Subjects inhaled 1.0 L of oxygen via a Tedlar bag from FRC before breath holding. These images were acquired by using a multisection balanced steady-state free precession sequence, and image location was copied from the preceding hyperpolarized ^{129}Xe MR imaging for coregistration purposes. Imaging parameters were as follows: 15-mm coronal sections covering the whole lung, 40 × 40-cm field of view, 128 × 128 matrix resolution, 125-kHz bandwidth, 1.2/2.8, and 45° flip angle.

Reproducibility of ^{129}Xe MR Imaging

A subgroup of patients returned within 6 weeks of initial baseline imaging for repeat hyperpolarized ^{129}Xe MR ventilation imaging to enable assessment of reproducibility. Reproducibility imaging was performed only in patients with stable disease who remained exacerbation free since the initial imaging examination (n = 11). Reproducibility hyperpolarized ^{129}Xe MR ventilation and anatomic proton MR images were obtained in the same way as previously described.

Figure 1

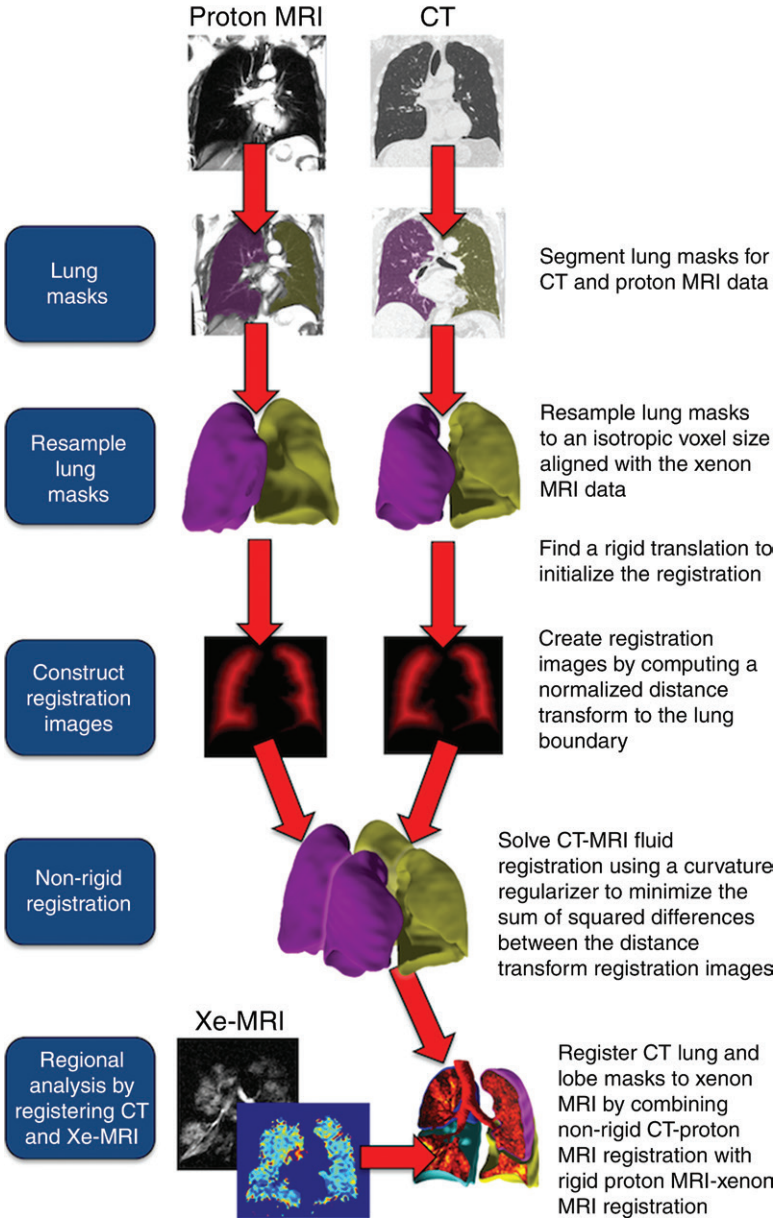

Figure 1: Schematic of pipeline for regional image analysis with PTK. Regional analysis is performed by registering lobar boundaries from CT to proton MR imaging by combining a nonrigid method from CT to proton MR imaging with a rigid translation from proton MR imaging to ^{129}Xe MR imaging.

MR Imaging Analysis

Analysis of hyperpolarized ^{129}Xe MR images was performed by using Pulmonary Toolkit (PTK) (17), an open-source image processing kit that runs in the Matlab environment (MathWorks, Natick, Mass). PTK builds on previous techniques developed in our group (18) and is capable of fully automated lobar analysis of hyperpolarized ^{129}Xe MR ventilation and diffusion-weighted imaging. Key steps in the pipeline involving PTK are illustrated in Figure 1). Regional analysis is performed by using image registration

to apply lung and lobar boundaries from CT data to ^{129}Xe MR images. Direct registration between CT and ^{129}Xe MR images is challenging owing to the difficulty in identifying lung boundaries and other anatomic features from ^{129}Xe MR imaging data. For this reason, registration is performed in two steps, with proton MR imaging as an intermediate stage. Proton MR imaging provides an ideal intermediate stage because the lung inflation protocol can be matched, which enables images to be rigidly registered to ^{129}Xe MR imaging data by using image meta-data, and the visible lung boundaries can be used to perform a nonrigid registration with CT data.

Hyperpolarized ^{129}Xe MR imaging ventilation and ADC data were saved into the image space for analysis. ADCs per pixel were calculated according to a published formula (10). PTK incorporates a graphical user interface that first completes automated segmentation of the lungs on CT and proton MR images and the lobes on CT data. The segmented lung masks are used to perform an intermodal registration that allows the CT lobe masks to be registered to proton and ^{129}Xe MR imaging. This enables the computation of lobar masks on proton MR images and, subsequently, ^{129}Xe MR images, which are then used to establish lobar ventilation and ADC maps. The accuracy of image registration was ensured by confirming a volume overlap index (Dice index) of more than 0.8.

The method for automated segmentation of the lungs from proton MR images comprises an initialization based on three-dimensional region growing with an adaptive threshold. Contour refinement is then performed for each coronal section by using a two-dimensional level-set algorithm with an image gradient force, a region-based speed term, and curvature regularization.

The algorithm used for automated CT lung segmentation is based on a region-growing method with a global threshold to extract the initial lung region (19), followed by left and right lung separation and boundary refinement (20)—both of which have been validated in the literature.

The automated algorithm for CT lobe segmentation combines a Hessian-based filter for detecting pulmonary fissures with anatomic cues from segmented lungs, airways, and pulmonary vessels. This method is robust to small vessels crossing the lobar boundary, requires no training or previous data, and is robust to incomplete fissures (21).

Registration between the CT and proton MR images is performed by first generating normalized distance transforms to the lung boundaries for each lung mask. A deformation field is computed by using curvature regularization to minimize the sum of squared differences between the normalized distance transforms for each modality. Nonlinear fluid registration of multimodality pulmonary imaging has been previously reported to be superior to rigid registration (22).

Quantitative CT

Quantitative CT was performed with a 16-section scanner (Discovery 670; GE Healthcare) as part of the patient's clinical work-up. Images were obtained 60 seconds after intravenous administration of contrast material with the following parameters: 1.25-mm-thick sections, 50–400 smart mA current, 120-kV voltage, 1.25-mm tube collimation, and 0.938 beam pitch.

Quantitative CT was performed during suspended inspiration after inhalation of 1.0-L oxygen via a Tedlar bag from FRC to ensure lung volumes were as similar to those at hyperpolarized ^{129}Xe MR imaging as possible. Subjects underwent breath-hold training by radiographer instruction to ensure reproducibility. No data were acquired in expiration.

Quantitative CT Analysis

Quantitative CT scans were analyzed by using PTK to determine percentage emphysema on a whole-lung and lobar basis. The extent of emphysema was assessed by using the %LAA.

Quantitative CT scans were also analyzed by using commercially available software (Thoracic VCAR; GE Healthcare) to measure average lumen diameter and wall area for third- to sixth-generation airways (Fig 2). To reduce technical errors associated with small airways, only those with an internal perimeter greater than 6 mm were included. To avoid potential intersubject bias from different airway size distributions, a standardized measure for airway wall thickness (Pi10) was derived for each subject by plotting the square root of airway wall area against the internal perimeter of each measured airway (23). The resulting regression line was used to calculate the square root of the bronchial wall area for a "theoretic airway" with an internal perimeter of 10 mm within each lobe (24). This method has been previously used and is described elsewhere (23).

Performance of PFTs

Subjects completed PFTs with a compact plus flowmeter pulmonary function testing station (Hypair; Medisoft Group, Sorinnes, Belgium) and a body plethysmography system (MasterScreen Body; Carefusion, Hoechberg, Germany). PFTs included spirometry (FEV_1, FEV_1/forced vital capacity) and plethysmography (residual volume expressed as a percentage of total lung capacity, FRC, and T_{LCO}). Individual recordings were compared with predicted values from standard published data.

Statistical Analysis

A priori analyses were completed to evaluate the relationship between imaging parameters and PFT results. The Pearson correlation coefficient was calculated between *(a)* ^{129}Xe MR imaging lobar parameters and quantitative CT–derived lobar %LAA, *(b)* ^{129}Xe MR imaging lobar parameters and quantitative CT–derived lobar Pi10, *(c)* whole-lung ^{129}Xe MR imaging parameters and PFT metrics, *(d)* whole-lung quantitative CT–derived %LAA and PFT metrics, and *(e)* whole-lung quantitative CT–derived Pi10 and PFT metrics.

For computation of lobar correlation coefficients, data from the five pulmonary lobes were included per patient. For ^{129}Xe MR ventilation imaging, 110 lobar pairs were included and for HP ^{129}Xe-MR diffusion-weight imaging, 105 lobar pairs were included. All inference (P values) were completed on a per-pair, not a per-patient, basis. $P <$

Figure 2

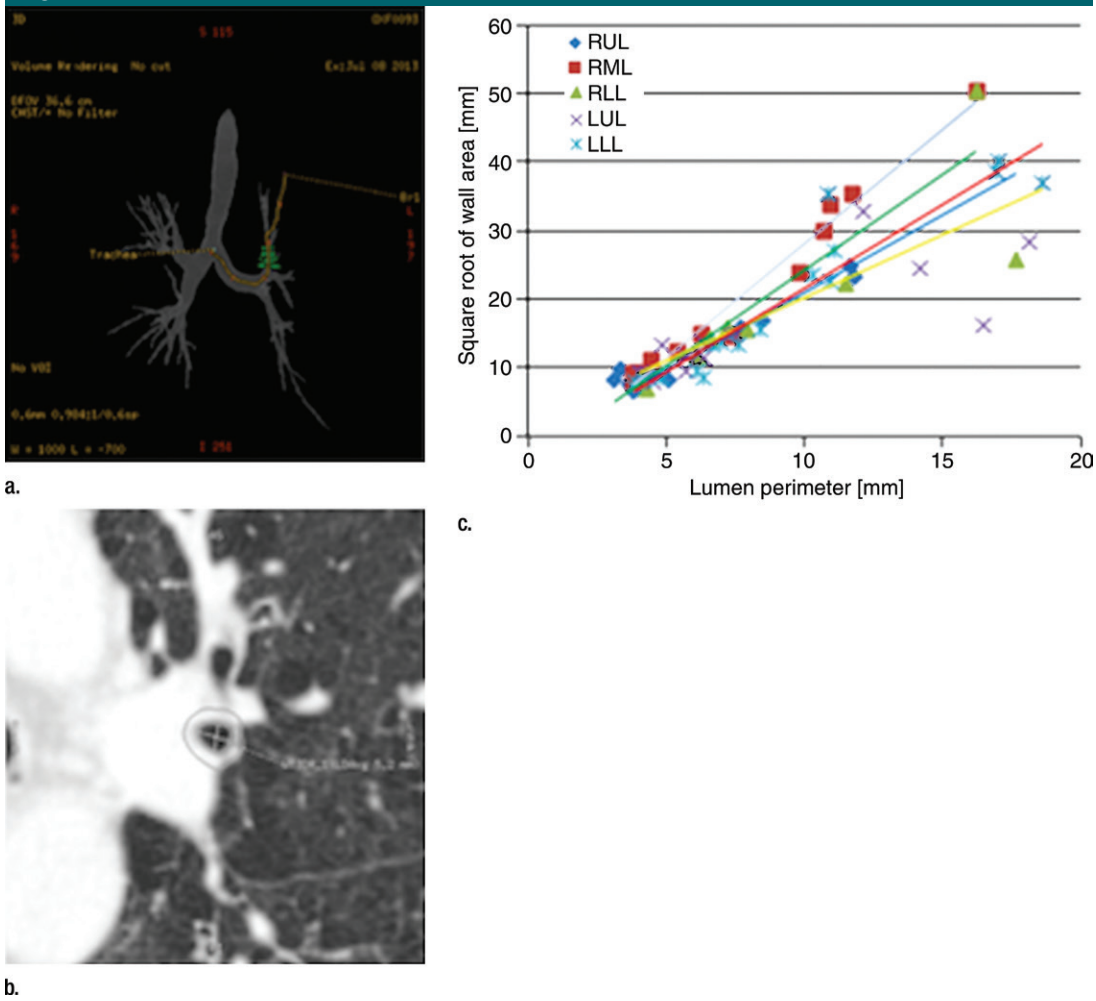

Figure 2: Method used to quantify lobar airway wall thickness from quantitative CT by using Pi10. **(a)** Image shows three-dimensional airway segmentation derived from volumetric CT data. **(b)** Axial CT image shows measurement of average airway diameter and wall area. **(c)** Regression line used to determine Pi10 for each lobe of lung. *LLL* = left lower lobe, *LUL* = left upper lobe, *RLL* = right lower lobe, *RML* = right middle lobe, *RUL* = right upper lobe.

.05 was considered indicative of a statistically significant difference.

Bland-Altman statistics were used to determine the reproducibility of ^{129}Xe MR ventilation imaging. The mean, standard deviation, mean difference, 95% limits of agreement, and coefficient of repeatability for ^{129}Xe MR lobar ventilated volume (in percentage) were established for the 11 patients who completed reproducibility imaging.

Results

Hyperpolarized ^{129}Xe MR imaging was well tolerated by all patients, with no serious adverse events. Hyperpolarized ^{129}Xe diffusion-weighted MR imaging was not performed in one patient owing to xenon coil failure. Data analysis for ^{129}Xe diffusion-weighted MR imaging was therefore completed in 21 patients. Images from ^{129}Xe MR ventilation imaging and quantitative CT were successfully obtained in all patients. Reproducibility ^{129}Xe MR ventilation imaging was completed in 11 patients. Example ^{129}Xe MR ventilation and diffusion-weighted images and data analyses are shown in Figures 3 and 4.

Lobar ^{129}Xe MR imaging percentage ventilated volume and lobar ^{129}Xe MR imaging average ADC showed correlation with lobar quantitative CT–derived %LAA ($r = -0.32$, $P < .001$ and $r = 0.75$, $P < .0001$, respectively) (Fig 5). There was no correlation between lobar ^{129}Xe MR imaging parameters and lobar quantitative CT Pi10 (Table 2).

Descriptive statistics for ^{129}Xe MR imaging– and quantitative CT–derived metrics according to pulmonary lobe are provided in Table 3.

Whole-lung ^{129}Xe MR imaging–derived average ADC showed moderate correlation with percentage predicted TLCO ($r = -0.61$, $P < .005$) and percentage predicted FRC ($r = 0.47$, $P < .05$).

Figure 3

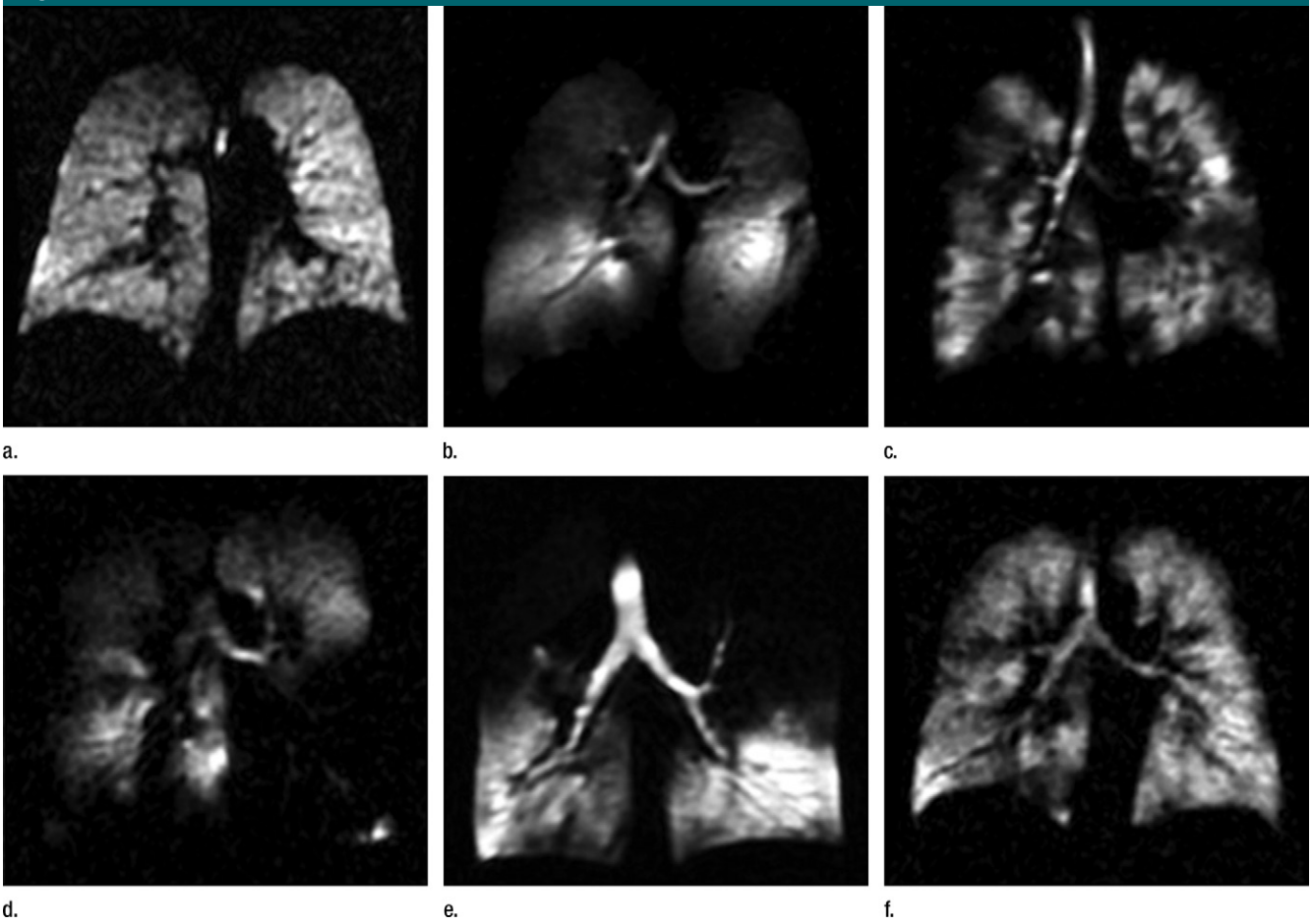

Figure 3: **(a)** Coronal hyperpolarized ^{129}Xe MR ventilation image in healthy volunteer shows homogeneous signal intensity distribution. **(b–f)** Coronal hyperpolarized ^{129}Xe MR ventilation images in patients with COPD demonstrate typical regions absent of signal intensity or of low signal intensity known as "ventilation defects" and corresponding to obstructed airflow.

Whole-lung quantitative CT–derived %LAA showed a similar correlation with percentage predicted TLCO ($r = -0.65$, $P < .005$) and near statistically significant correlation with percentage predicted FRC ($r = 0.39$, $P = .072$). There was poor correlation between whole-lung ^{129}Xe MR imaging–derived percentage ventilated volume and PFT metrics (Table 4). There was a similar weak correlation between whole-lung quantitative CT–derived Pi10 and PFT metrics ($r = -0.34$ to 0.24, $P = .13$–$.86$) (Table 4). There was no correlation between any imaging parameters and spirometric indexes ($r = -0.37$ to 0.24, $P = .092$–$.29$) (Table 4).

The Bland-Altman plots of agreement (Fig 6) show the majority of differences between repeated lobar ^{129}Xe MR ventilated volume percentage measurements to lie within the 95% limits of agreement. There are two outliers. Reproducibility statistics calculated from paired hyperpolarized ^{129}Xe MR ventilation imaging included the mean lobar ventilated volume percentage ± standard deviation (77.12% ± 1 6.55), the mean difference (5.63%, 95% limits of agreement: −12.43% to 23.69%), and the coefficient of repeatability (18.06).

Discussion

In this study, we generated lobar ventilation and ADC measurements by using hyperpolarized ^{129}Xe MR imaging and demonstrated moderate correlation with lobar lung anatomy (quantitative CT) and global functional transfer capability (TLCO). Although previous studies have shown the feasibility of hyperpolarized gas imaging to determine global functional parameters of the lung, translation of this technique from academic to routine clinical application has been limited to date. Accurate lobar quantification of hyperpolarized ^{129}Xe MR imaging is particularly relevant to the field of respiratory medicine with emerging regional treatments not adequately assessed with standard whole-lung methods. These ^{129}Xe MR imaging lobar analyses offer the potential for

Figure 4

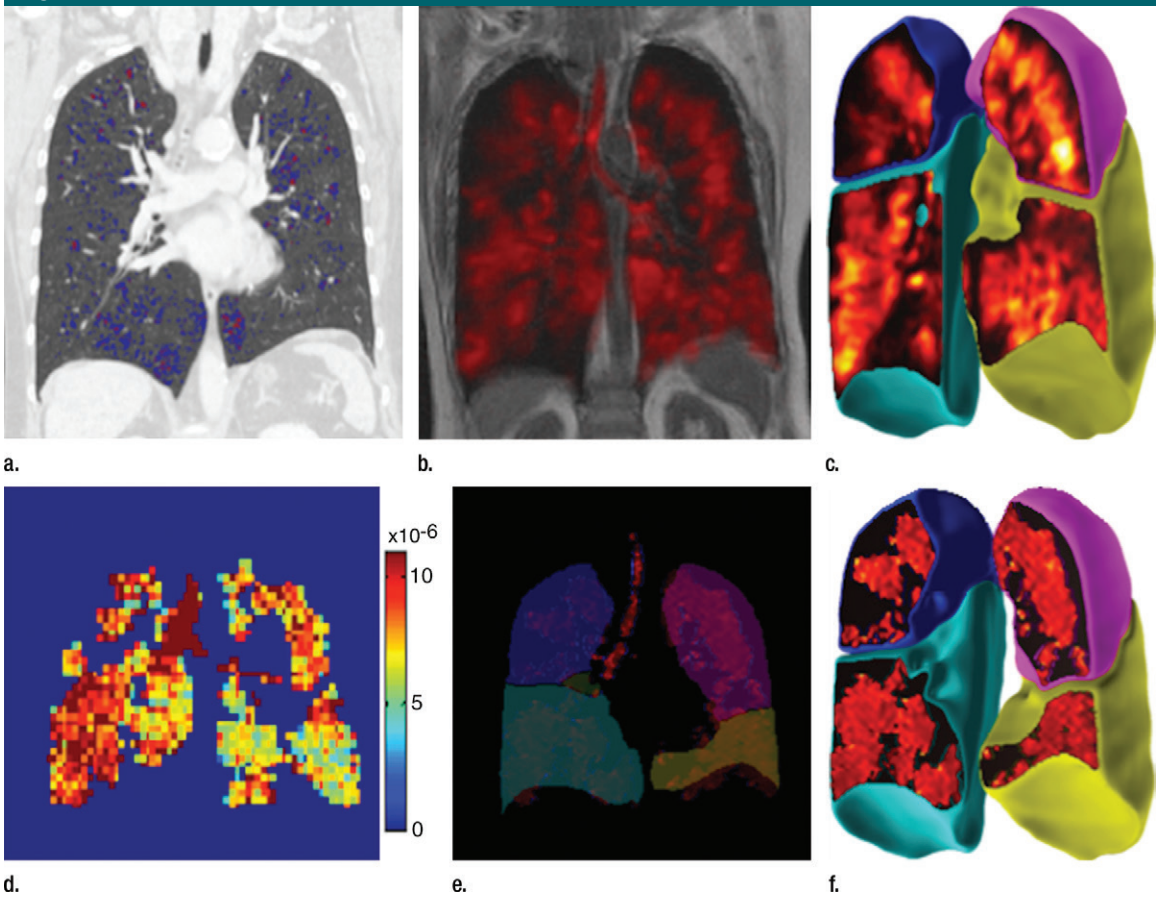

Figure 4: Data analysis of coronal quantitative CT scans and hyperpolarized ^{129}Xe ventilation and diffusion-weighted MR images in patient with COPD. **(a)** Emphysema density map from quantitative CT. Colored regions correspond to lung voxels with attenuation less than −950 HU. **(b)** Hyperpolarized ^{129}Xe MR ventilation image coregistered to proton MR image. **(c)** Three-dimensional hyperpolarized ^{129}Xe MR image of lobar ventilation. **(d)** Hyperpolarized ^{129}Xe MR imaging–derived ADC map ($\times 10^{-6}$ m^2/sec). **(e)** Hyperpolarized ^{129}Xe MR imaging–derived ADC map coregistered to segmented lobes from quantitative CT. **(f)** Three-dimensional hyperpolarized ^{129}Xe MR imaging–derived lobar ADC map.

improved description of COPD regional functional heterogeneity and assessment for regional treatments such as lung volume reduction surgery or endobronchial valve placement. Unlike CT, hyperpolarized ^{129}Xe MR imaging does not expose patients to radiation and may also be performed repeatedly, potentially immediately after an intervention to determine its efficacy. This may enable early treatment modifications or allow clinicians to inform patients of the likely success of their intervention.

The feasibility of regional ventilation including lobar measures with ^{3}He MR imaging in healthy volunteers and subjects with asthma has been reported (15,16), but, to our knowledge, lobar ventilation and ADC measures with use of hyperpolarized ^{129}Xe MR imaging have not been previously determined. In this study, we derived ventilation and ADC values per lobe with ^{129}Xe MR imaging after automated nonrigid registration to proton MR imaging and quantitative CT. The software used to generate lobar ^{129}Xe MR imaging measures has a graphical user interface that offers the potential for incorporation into the clinical workflow and making the technique translatable to other respiratory centers. Furthermore, lobar ^{129}Xe MR imaging measures could be used to evaluate treatment in other obstructive diseases, for example lobar hyperpolarized ^{129}Xe MR imaging–derived ADCs in patients with α_1-antitrypsin deficiency and lobar hyperpolarized ^{129}Xe MR imaging–derived ventilated volume percentage in patients with asthma. This work may also enable the stratification of patients and help determine suitability for specific regional pulmonary treatments.

The lobar percentage ventilated volumes and average lobar ADC values as assessed with hyperpolarized ^{129}Xe MR imaging showed statistically significant correlation with quantitative CT–derived emphysema. These findings are consistent with those from the study by Kirby et al (25), who investigated hyperpolarized ^{3}He MR imaging and hyperpolarized ^{129}Xe MR ventilation

Figure 5

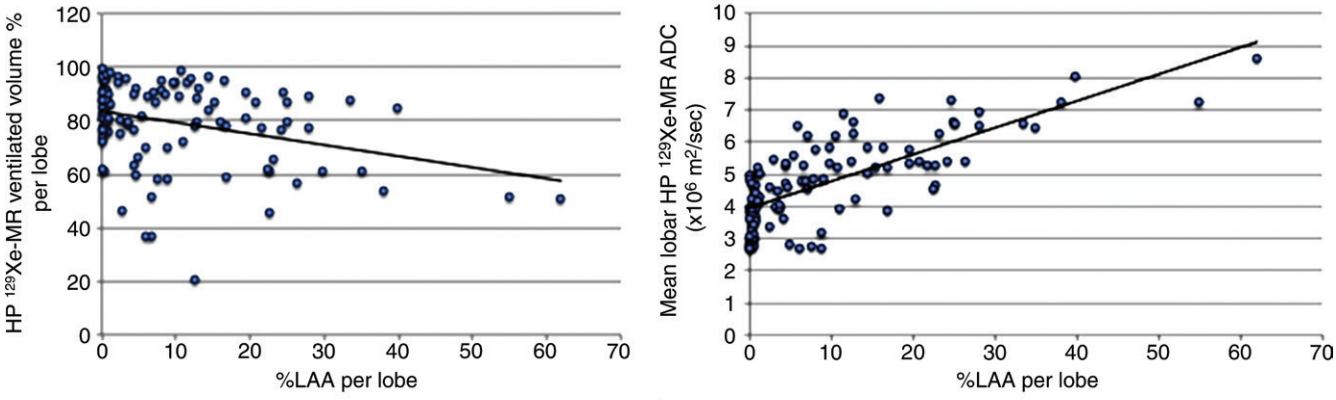

Figure 5: Scatter plots show correlation between lobar imaging parameters. **(a)** Linear correlation between hyperpolarized *(HP)* ^{129}Xe MR imaging–derived ventilated volume and %LAA per pulmonary lobe. **(b)** Linear correlation between hyperpolarized *(HP)* ^{129}Xe MR imaging–derived mean ADC and %LAA per pulmonary lobe.

Table 2

Pearson Correlation of Lobar Imaging Parameters

Parameter	^{129}Xe MR Imaging–derived Ventilated Volume	^{129}Xe MR Imaging–derived Average ADC*
Quantitative CT–derived %LAA	−0.32 (.00061)	0.75 (7.7×10^{-20})
Quantitative CT–derived Pi10	−0.086 (.38)	−0.051 (.61)

Note.—Data are correlation coefficients, with *P* values in parentheses.

* Data are available for only 21 patients.

imaging in 10 subjects with COPD and showed significant correlation between regions of decreased hyperpolarized ^{129}Xe MR imaging–derived ventilation with quantitative CT–derived emphysema but not quantitative CT–derived airway wall measurement. Significant correlation between hyperpolarized ^{3}He MR imaging–derived ADC and quantitative CT–derived emphysema has been similarly reported (26). The relationship between whole-lung hyperpolarized ^{129}Xe MR imaging–derived ADC and quantitative CT–derived emphysema in healthy volunteers and patients with COPD has also been demonstrated (27). Our results confirm these findings and extend correlations between hyperpolarized ^{129}Xe MR imaging and quantitative CT on a lobar level.

The whole-lung average ADCs from our study population are consistent with those from the study by Kaushik et al (10), who reported a mean ADC of 0.056 $cm^2\ sec^{-1} \pm 0.008$ for patients with COPD and emphysema. Whole-lung average ADCs from our patients with COPD correlated with percentage predicted T_{LCO} and percentage predicted FRC. Whole-lung quantitative CT–derived emphysema showed a similar correlation with T_{LCO}, providing evidence that hyperpolarized ^{129}Xe MR imaging–derived ADC measurements reflect emphysematous destruction of the pulmonary microstructure. The relationship between hyperpolarized gas MR imaging–derived ADC, quantitative CT–derived emphysema, and T_{LCO} is established in patients with and patients without COPD (26,28), in keeping with our results.

We did not demonstrate a correlation between spirometric indexes and hyperpolarized ^{129}Xe MR imaging measurements. A possible explanation may be that ^{129}Xe MR imaging provides regional measurements of lung function, accounts for disease heterogeneity, and can be easily performed at the same lung volume for all patients, that is, FRC plus 1.0 L of hyperpolarized ^{129}Xe gas. Conversely, spirometry only provides a global measure of lung function and depends on external factors including patient effort, which may confound results. There are conflicting reports within the literature regarding the relationship between hyperpolarized gas imaging and spirometry. Woodhouse et al (29) showed no relationship between hyperpolarized ^{3}He MR ventilation imaging and spirometry. Other investigators have reported a significant correlation between spirometry and hyperpolarized ^{129}Xe and ^{3}He MR imaging–derived ventilation defect percentage (27,30). Similarly, contrasting significant correlations (31) and weak associations (30) between hyperpolarized ^{3}He MR imaging–derived ADC and spirometric measurements are published in the literature. These discrepant results may be explained by the relatively small sample sizes included, the varying patient disease severity, and nonstandardized analysis methods ranging from manual to semiautomated segmentation.

There was no correlation between quantitative CT–derived Pi10 and other imaging parameters or spirometric measurements in our cohort. The small peripheral airways (<2 mm in

Table 3

Descriptive Statistics of Imaging Parameters according to Pulmonary Lobe

Parameter	RUL	RML	RLL	LUL	LLL
^{129}Xe MR imaging–derived ventilated volume (%)	74.81 ± 13.94	85.52 ± 11.25	79.06 ± 19.59	76.88 15.51	80.67 ± 13.29
^{129}Xe MR imaging–derived average ADC ($\times 10^{-6}$ m^2/sec)*	5.05 ± 1.41	4.52 ± 1.12	4.66 ± 1.25	4.98 ± 1.50	4.55 ± 1.26
Quantitative CT–derived %LAA†	6.62 (0.84, 21.89)	7.06 (0.50, 12.03)	4.05 (0.45, 11.81)	6.90 (1.11, 15.87)	3.20 (0.41, 9.3)
Quantitative CT–derived Pi10 (mm)	6.17 ± 0.92	6.82 ± 2.06	6.42 ± 1.14	6.04 ± 0.96	5.84 ± 0.97

Note.—Except where indicated, data are means ± standard deviations. LLL = left lower lobe, LUL = left upper lobe, RLL = right lower lobe, RML = right middle lobe, RUL = right upper lobe.

* Data are available for only 21 patients.

† Numbers in parentheses are the 25th and 75th percentiles.

Table 4

Pearson Correlation of Whole-Lung Imaging and PFT Parameters

PFT Parameter	^{129}Xe MR Imaging–derived Ventilated Volume	^{129}Xe MR Imaging–derived Average ADC*	Quantitative CT–derived %LAA	Quantitative CT–derived Pi10
FEV_1†	0.082 (.72)	−0.15 (.51)	−0.20 (.37)	0.24 (.29)
FEV_1/FVC	0.097 (.67)	−0.37 (.092)	−0.22 (.32)	0.040 (.86)
RV/TLC	−0.12 (.59)	−0.094 (.68)	−0.052 (.82)	−0.27 (.23)
FRC†	0.11 (.64)	0.47 (.026)	0.39 (.072)	−0.34 (.13)
T_{LCO}†	0.14 (.52)	−0.61 (.0024)	−0.65 (.0012)	0.13 (.56)

Note.—Data are correlation coefficients, with *P* values in parentheses. FEV_1 is the prebronchodilator value. FVC = forced expiratory vital capacity, RV/TLC = residual volume expressed as percentage of total lung capacity.

* Data are available for only 21 patients.

† Percentage predicted.

Figure 6

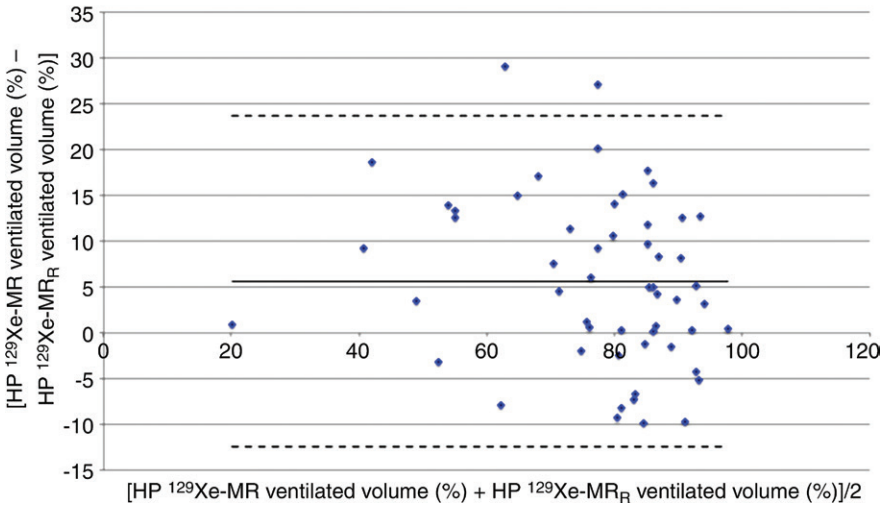

Figure 6: Bland-Altman agreement plot shows reproducibility of lobar hyperpolarized *(HP)* ^{129}Xe MR imaging–derived ventilated volume generated with automated PTK analysis tool acquired in 11 patients. Solid line indicates mean absolute difference. Dashed lines represent 95% confidence interval of mean difference (limits of agreement).

diameter) are attributed to the site of airflow limitation in COPD but are not readily resolved on CT scans. Previous pathology studies have shown that the disease process occurring in COPD affects both large and small airways and, as such, measurements of large airways at quantitative CT could reflect the state of small airways (32). Nakano et al (33) supported this hypothesis by showing correlation of quantitative CT–derived airway dimensions of the upper lobe segmental bronchus with spirometry (33) and histologic examination (34). However, it has been reported that emphysema weakens the relationship between FEV_1 and quantitative CT–derived peripheral airway wall measurements (35). Emphysema may cause a loss of airway tethering, attenuating peripheral airway dilatation during inspiration (36) and subsequently reducing the accuracy of quantitative CT–derived airway wall measurements. It is plausible that Pi10, a measure derived from predominantly larger airways, may not accurately reflect the smaller peripheral airways in the presence of emphysema, which would explain why this parameter did not correlate with spirometric or hyperpolarized ^{129}Xe MR imaging measurement in our cohort. Furthermore, evaluation of more than 4000 smokers with and without COPD showed poor correlation of Pi10 with spirometry and quantitative CT–derived emphysema (37), which is consistent with our current findings.

This study has a number of limitations. Despite the relatively small sample size, our study cohort included subjects that comprise most clinically

relevant COPD cases (Global Initiative for Chronic Obstructive Lung Disease stage II–IV). Future work should include patients with milder COPD (Global Initiative for Chronic Obstructive Lung Disease stage I) to identify lobar abnormalities for early stage disease. The proton MR images, hyperpolarized ^{129}Xe MR ventilation and ADC images, and quantitative CT scans were acquired during separate breath holds. Despite the acquisition of all images after inhalation of 1.0 L from FRC, potential lung volume differences may have arisen as a result of subjects varying the amount of air exhaled to achieve FRC before inhalation for each breath hold. Potential lung volume differences and body movement may have affected accurate image registration, although the nonrigid multimodal registration performed by PTK corrects for this. The requirement for coregistration might be reduced in future studies by simultaneous acquisition of proton and hyperpolarized ^{129}Xe MR imaging during a single breath hold (38). The software used for image data analysis (PTK) is open source and not currently available commercially. Further optimization of the software would be required before integration into the clinical workflow is possible. Another limitation of the study is that comparison between hyperpolarized ^{129}Xe MR imaging and other emerging functional lung imaging techniques was not performed (eg, comparison with oxygen-enhanced and fluorine 19 MR imaging).

In conclusion, lobar measures have been derived with hyperpolarized ^{129}Xe MR ventilation and diffusion-weighted imaging by using automated nonrigid coregistration and were shown to correlate with lobar lung anatomy (at quantitative CT) and global functional transfer capability (T_{LCO}). Future work is needed to determine if lobar hyperpolarized ^{129}Xe MR imaging–derived ventilation and ADC measurements provide an improved method for selecting patients for regional lung treatments and whether they offer new insights into regional lung treatment efficacy in patients with COPD and other obstructive lung diseases.

Acknowledgments: We acknowledge Tara Harris-Wright and Andrea Byles for their kind help with patient recruitment and supervision. We also thank Anthony McIntyre, Kenneth Jacob, and Jennifer Lee for their technical assistance.

Disclosures of Conflicts of Interest: T.N.M. disclosed no relevant relationships. **N.R.** disclosed no relevant relationships. **A.H.N.** disclosed no relevant relationships. **M.C.** disclosed no relevant relationships. **X.X.** disclosed no relevant relationships. **N.J.S.** disclosed no relevant relationships. **T.D.** disclosed no relevant relationships. **V.G.** disclosed no relevant relationships. **J.M.W.** Activities related to the present article: disclosed no relevant relationships. Activities not related to the present article: is a paid consultant for Novartis; institution has grants/grants pending from Novartis, GSK, and GE; receives payment for lectures including service on speakers bureaus from Boehringer. Other relationships: disclosed no relevant relationships. **F.V.G.** disclosed no relevant relationships.

References

1. Global Initiative for Chronic Obstructive Lung Disease (GOLD). Global strategy for the diagnosis, management and prevention of COPD. http://www.goldcopd.org/. Published 2015. Accessed May 2, 2015.
2. Lopez AD, Shibuya K, Rao C, et al. Chronic obstructive pulmonary disease: current burden and future projections. Eur Respir J 2006;27(2):397–412.
3. Celli BR, Cote CG, Marin JM, et al. The body-mass index, airflow obstruction, dyspnea, and exercise capacity index in chronic obstructive pulmonary disease. N Engl J Med 2004;350(10):1005–1012.
4. Driehuys B, Martinez-Jimenez S, Cleveland ZI, et al. Chronic obstructive pulmonary disease: safety and tolerability of hyperpolarized ^{129}Xe MR imaging in healthy volunteers and patients. Radiology 2012;262(1):279–289.
5. Shukla Y, Wheatley A, Kirby M, et al. Hyperpolarized ^{129}Xe magnetic resonance imaging: tolerability in healthy volunteers and subjects with pulmonary disease. Acad Radiol 2012;19(8):941–951.
6. Fain S, Schiebler ML, McCormack DG, Parraga G. Imaging of lung function using hyperpolarized helium-3 magnetic resonance imaging: review of current and emerging translational methods and applications. J Magn Reson Imaging 2010;32(6):1398–1408.
7. Mugler JP 3rd, Altes TA. Hyperpolarized ^{129}Xe MRI of the human lung. J Magn Reson Imaging 2013;37(2):313–331.
8. van Beek EJ, Wild JM, Kauczor HU, Schreiber W, Mugler JP III, de Lange EE. Functional MRI of the lung using hyperpolarized 3-helium gas. J Magn Reson Imaging 2004;20(4):540–554.
9. Svenningsen S, Kirby M, Starr D, et al. Hyperpolarized (3) He and (129) Xe MRI: differences in asthma before bronchodilation. J Magn Reson Imaging 2013;38(6):1521–1530.
10. Kaushik SS, Cleveland ZI, Cofer GP, et al. Diffusion-weighted hyperpolarized ^{129}Xe MRI in healthy volunteers and subjects with chronic obstructive pulmonary disease. Magn Reson Med 2011;65(4):1154–1165.
11. de Lange EE, Altes TA, Patrie JT, et al. Evaluation of asthma with hyperpolarized helium-3 MRI: correlation with clinical severity and spirometry. Chest 2006;130(4):1055–1062.
12. Mathew L, Kirby M, Etemad-Rezai R, Wheatley A, McCormack DG, Parraga G. Hyperpolarized ^{3}He magnetic resonance imaging: preliminary evaluation of phenotyping potential in chronic obstructive pulmonary disease. Eur J Radiol 2011;79(1):140–146.
13. Kirby M, Heydarian M, Svenningsen S, et al. Hyperpolarized ^{3}He magnetic resonance functional imaging semiautomated segmentation. Acad Radiol 2012;19(2):141–152.
14. Tustison NJ, Avants BB, Flors L, et al. Ventilation-based segmentation of the lungs using hyperpolarized (3)He MRI. J Magn Reson Imaging 2011;34(4):831–841.
15. Tahir BA, Van Holsbeke C, Ireland RH, et al. Comparison of CT-based lobar ventilation with 3He MR imaging ventilation measurements. Radiology 2016;278(2):585–592.
16. Thomen RP, Sheshadri A, Quirk JD, et al. Regional ventilation changes in severe asthma after bronchial thermoplasty with (3)He MR imaging and CT. Radiology 2015;274(1):250–259.
17. Doel T. Pulmonary Toolkit. https://github.com/tomdoel/pulmonarytoolkit. Accessed May 23, 2015.
18. Plotkowiak M. Hyperpolarised gas MRI as a promising technique for regional chronic lung diseases assessment [thesis]. Oxford, England: University of Oxford, 2010.
19. Hu S, Hoffman EA, Reinhardt JM. Automatic lung segmentation for accurate quantitation of volumetric x-ray CT images. IEEE Trans Med Imaging 2001;20(6):490–498.
20. Kuhnigk JM, Dicken V, Zidowitz S, et al. Informatics in radiology (infoRAD): new tools for computer assistance in thoracic CT. I. Functional analysis of lungs, lung lobes, and bronchopulmonary segments. RadioGraphics 2005;25(2):525–536.
21. Doel T, Matin TN, Gleeson FV, Gavaghan DJ, Grau V. Pulmonary lobe segmentation

from CT images using fissureness, airways, vessels, and multilevel B-splines. Presented at the IEEE International Symposium on Biomedical Imaging, Barcelona, Spain, May 2–5, 2012.

22. Murphy K, van Ginneken B, Reinhardt JM, et al. Evaluation of registration methods on thoracic CT: the EMPIRE10 challenge. IEEE Trans Med Imaging 2011;30(11):1901–1920.
23. Grydeland TB, Dirksen A, Coxson HO, et al. Quantitative computed tomography: emphysema and airway wall thickness by sex, age and smoking. Eur Respir J 2009;34(4):858–865.
24. Patel BD, Coxson HO, Pillai SG, et al. Airway wall thickening and emphysema show independent familial aggregation in chronic obstructive pulmonary disease. Am J Respir Crit Care Med 2008;178(5):500–505.
25. Kirby M, Svenningsen S, Kanhere N, et al. Pulmonary ventilation visualized using hyperpolarized helium-3 and xenon-129 magnetic resonance imaging: differences in COPD and relationship to emphysema. J Appl Physiol (1985) 2013;114(6):707–715.
26. Diaz S, Casselbrant I, Piitulainen E, et al. Validity of apparent diffusion coefficient hyperpolarized 3He-MRI using MSCT and pulmonary function tests as references. Eur J Radiol 2009;71(2):257–263.
27. Kirby M, Svenningsen S, Owrangi A, et al. Hyperpolarized ^{3}He and ^{129}Xe MR imaging in healthy volunteers and patients with chronic obstructive pulmonary disease. Radiology 2012;265(2):600–610.
28. Kirby M, Owrangi A, Svenningsen S, et al. On the role of abnormal DLco in ex-smokers without airflow limitation: symptoms, exercise capacity and hyperpolarised helium-3 MRI. Thorax 2013;68(8):752–759.
29. Woodhouse N, Wild JM, Paley MN, et al. Combined helium-3/proton magnetic resonance imaging measurement of ventilated lung volumes in smokers compared to never-smokers. J Magn Reson Imaging 2005;21(4):365–369.
30. Kirby M, Mathew L, Wheatley A, Santyr GE, McCormack DG, Parraga G. Chronic obstructive pulmonary disease: longitudinal hyperpolarized ^{3}He MR imaging. Radiology 2010;256(1):280–289.
31. Salerno M, de Lange EE, Altes TA, Truwit JD, Brookeman JR, Mugler JP III. Emphysema: hyperpolarized helium 3 diffusion MR imaging of the lungs compared with spirometric indexes—initial experience. Radiology 2002;222(1):252–260.
32. Tiddens HA, Paré PD, Hogg JC, Hop WC, Lambert R, de Jongste JC. Cartilaginous airway dimensions and airflow obstruction in human lungs. Am J Respir Crit Care Med 1995;152(1):260–266.
33. Nakano Y, Muro S, Sakai H, et al. Computed tomographic measurements of airway dimensions and emphysema in smokers. Correlation with lung function. Am J Respir Crit Care Med 2000;162(3 Pt 1):1102–1108.
34. Nakano Y, Wong JC, de Jong PA, et al. The prediction of small airway dimensions using computed tomography. Am J Respir Crit Care Med 2005;171(2):142–146.
35. Yahaba M, Kawata N, Iesato K, et al. The effects of emphysema on airway disease: correlations between multi-detector CT and pulmonary function tests in smokers. Eur J Radiol 2014;83(6):1022–1028.
36. Diaz AA, Come CE, Ross JC, et al. Association between airway caliber changes with lung inflation and emphysema assessed by volumetric CT scan in subjects with COPD. Chest 2012;141(3):736–744.
37. Schroeder JD, McKenzie AS, Zach JA, et al. Relationships between airflow obstruction and quantitative CT measurements of emphysema, air trapping, and airways in subjects with and without chronic obstructive pulmonary disease. AJR Am J Roentgenol 2013;201(3):W460–W470.
38. Wild JM, Ajraoui S, Deppe MH, et al. Synchronous acquisition of hyperpolarised ^{3}He and ^{1}H MR images of the lungs: maximising mutual anatomical and functional information. NMR Biomed 2011;24(2):130–134.